Resilient Cities and Structures 2 (2023) 19–29

Contents lists available at ScienceDirect

Resilient Cities and Structures

journal homepage: www.elsevier.com/locate/rcns

Full Length Article

Designing resilient and economically viable water distribution systems: A Multi-dimensional approach

Beatrice Cassottana [a,*], Srijith Balakrishnan [a], Nazli Yonca Aydin [c], Giovanni Sansavini [b]

[a] Singapore-ETH Centre, 1 Create Way, CREATE Tower 06-01, 138602 Singapore
[b] ETH Zürich, Reliability and Risk Engineering, Leonhardstrasse 21, Zürich 8092, Switzerland
[c] Delft University of Technology, Faculty of Technology, Policy and Management, Jaffalaan 5, BX Delft 2628, Netherlands

ARTICLE INFO

Keywords:
Resilience
Economic analysis
Water distribution system
Interdependency
Recovery strategy

ABSTRACT

Enhancing the resilience of critical infrastructure systems requires substantial investment and entails trade-offs between environmental and economic benefits. To this aim, we propose a methodological framework that combines resilience and economic analyses and assesses the economic viability of alternative resilience designs for a Water Distribution System (WDS) and its interdependent power and transportation systems. Flow-based network models simulate the interdependent infrastructure systems and Global Resilience Analysis (GRA) quantifies three resilience metrics under various disruption scenarios. The economic analysis monetizes the three metrics and compares two resilience strategies involving the installation of remotely controlled shutoff valves. Using the Micropolis synthetic interdependent water-transportation network as an example, we demonstrate how our framework can guide infrastructure stakeholders and utility operators in measuring the value of resilience investments. Overall, our approach highlights the importance of economic analysis in designing resilient infrastructure systems.

1. Introduction

Water Distribution Systems (WDSs) are critical infrastructures that support human life and activities. Currently, scarce water resources and pipe leaks stress the water distribution infrastructure and impair its ability to satisfy customers demand in several areas of the world [1]. Furthermore, WDSs are exposed to climate-related extreme events, resulting in frequent and high-impact disruptions. The effects of such disruptions are further aggravated by the presence of interdependencies among critical infrastructure systems. For example, in the interdependent power-water-transportation network, a failure of a power generator could cut supply to and fail water pumps; congested roads result in longer travel times for the repair crew and, therefore, in delayed repairs of infrastructure components.

Traditional risk assessment approaches, which rely upon the identification of hazards and the development of subsequent test scenarios, fall short in identifying high-impact climate-related extreme events. In this context, resilience assessment has emerged to fill the gap of reacting to unexpected and unforeseen events [2]. Although there is no unanimously accepted definition of resilience and state-of-the-art of resilience assessment is far from consolidated [3–5], authors have recognized the multidimensional and complex nature of resilience [6,7], which needs to be addressed by appropriate resilience metrics.

In order to improve system resilience, water utilities around the world are taking action to limit network losses by implementing leak detection and repair systems [8,9]. Specifically, Supervisory Control and Data Acquisition (SCADA) systems are being increasingly deployed to detect water leakages and isolate the failed components through the use of sensors, controllers and actuators [10,11]. While SCADA systems have been shown to effectively reduce water loss and secure water supply during disruptions [12,13], they involve considerable investments for the installation of monitoring and controlling technologies, which must be justified by significant benefits. Therefore, assessing resilience exclusively based on the resilience triangle paradigm, i.e., the integral over time of the performance loss [2], does not suffice, but the environmental costs and economic losses associated with the disruption must also be quantified [14].

In this study, we develop a methodological framework to assess the resilience of a WDS under disruption scenarios of increasing magnitude and assess the economic viability of resilience strategies corresponding to the installation of remotely-controlled shutoff valves. Specifically, in order to deal with unknown threats, the Global Resilience Analysis (GRA) approach is adopted to analyze system resilience under any com-

* Corresponding author.
E-mail addresses: beatrice.cassottana@sec.ethz.ch (B. Cassottana), srijith.balakrishnan@sec.ethz.ch (S. Balakrishnan), N.Y.Aydin@tudelft.nl (N.Y. Aydin), sansavig@ethz.ch (G. Sansavini).

https://doi.org/10.1016/j.rcns.2023.05.004
Received 17 November 2022; Received in revised form 8 May 2023; Accepted 18 May 2023

bination of component failures [15,16]. GRA relies on the identification of stress-strain curves, in which the stress corresponds to the number of failed components, irrespective of the triggering hazard, and the strain to the resulting resilience metric. In order to address the multidimensional nature of resilience, three metrics are considered to quantify the performance loss in terms of (1) water demand not satisfied, (2) water loss and (3) energy consumed during the disruption. Therefore, an economic analysis is conducted to quantify the trade-offs between the investment costs of resilience strategies and the potential cost savings deriving from their implementation.

Different from previous studies, WDS behaviour over time, including performance loss and recovery, is modeled using an integrated water and transportation simulation platform consisting of a pressure-dependent hydraulic simulation model and a static traffic assignment model. The framework is exemplified with reference to the synthetic city of Micropolis [17].

2. Background

2.1. Multidimensional resilience assessment

The definition of resilience has evolved over time. One of the first definitions of resilience was coined by Holling, who defined resilience as the ability to absorb change and disturbance without losing core functionalities [18]. While this definition applied to ecological systems, the same acceptation of resilience was later applied to infrastructure systems. In this regard, in their seminal paper, Bruneau and his co-authors [2] defined resilience from an engineering perspective as consisting of four capacities (i.e., robustness, redundancy, resourcefulness, rapidity) and proposed the resilience triangle paradigm, i.e., the integral over time of the performance loss, as resilience metric. In the last decades, a multitude of resilience definitions and metrics have emerged in the literature [4,5], which include different system capacities and associated metrics [3,19].

Although state-of-the-art of resilience is far from consolidated, authors have recognized the multidimensional and complex nature of resilience. Specifically, authors have highlighted the trade-offs between resilience goals across different temporal and spatial scales [20–22]. For example, short-term resilience goals, which seek to maximize redundancy and diversity, may conflict with sustainability goals, which aim to maximize efficiency and ensure resilience in the long-term [23]. The traditional view on resilience, intended as the capacity of a system to bounce back after a disruption [24], needs to be integrated with sustainability principles, which prescribe the distributional equity of resources across generations and populations [22,25]. At the same time, resilience assessment, which is based on the quantification of the performance lost by the system during the disruption [2], needs to integrate economic, environmental and social dimensions.

2.2. Economic analysis of WDSs

Previous literature conducted economic analyzes of WDSs to identify the best WDS design. Creaco and co-authors [8], for example, compared the benefits of conventional pressure-reducing valves versus remotely real-time valves considering three scenarios of leakage. The last announced Battle of the Water Networks [26] - a competition related to the design and operation of WDSs - calls for solutions to limit leaks and non-revenue water in order to ensure continuous water supply. Similarly, previous battles called for water network designs that minimize costs while ensuring demand satisfaction [27,28]. To answer these calls, optimization methods were used to find optimal WDS designs that ensure water service availability (reliability) while minimizing costs [29–31]. However, these studies do not consider WDS performance under extreme disruptive events and therefore lack design for resilience [32].

Another stream of literature evaluated the direct economic damage of water network disruptions. Zhou and co-authors [33], for example, developed a framework to conduct a cost-benefit analysis of various adaptation options for an urban drainage system subject to flooding under different climate change scenarios. The authors used national damage cost databases to estimate the economic losses associated with increasing levels of flooding. In other studies, pre-defined fragility curves were used to estimate the probability of failure of a network component subject to increasing seismic events [34,35]. Therefore, economic losses were directly associated with the failed components [35,36] or with the corresponding loss of service computed using simplistic models [37]. While these studies advanced the understanding of resilience by quantifying the direct costs associated with water network disruptions, they do not explicitly model the hydraulic behavior of the water network, thus failing to capture the cascading effects of component failures within the network and the resulting loss of system performance.

3. Methods

The methodological framework adopted in this study is illustrated in Fig. 1. The framework consists of two parts: (1) modeling and simulation (in blue in the figure) and (2) evaluation and analysis (in orange).

In the first part, an infrastructure model is developed to simulate the performance of the interdependent WDS and road transportation network as described in Section 3.1.1. Disruption scenarios of increasing magnitude are modeled for the water network by increasing the number of failed pipes (i) from 0 to the total number of pipes exposed to a given hazard (N). For a given disruption magnitude, a sampling strategy is implemented as explained in Section 3.1.2 and the number of simulations (N_i) computed for each i-level. Finally, a resilience strategy (s) is implemented by modifying the WDS structure. Therefore, recovery is modeled by ranking the failed pipes according to a pre-selected criterion corresponding to a given strategy s and updating the infrastructure model with the repaired pipes as described in Section 3.1.3.

In the second part of the framework, three metrics, namely the total performance loss, the total water loss and the additional energy consumed (see Section 3.2.1), are defined and computed to assess the WDS performance under various disruption and recovery scenarios. Therefore, an economic analysis is conducted as described in Section 5.3 to evaluate the expected annual costs corresponding to each resilience strategy.

3.1. Modeling and simulation

3.1.1. Interdependent infrastructure model

The interdependent infrastructure model consists of a model for the WDS and a model for the road traffic network. The WDS model includes a module to run hydraulic simulations using the WNTR Simulator of the Water Network Tool for Resilience (WNTR) [38]. WNTR allows for pressure-dependent analysis [39,40], in which the satisfied demand $d(t)$ is computed using the demand-pressure relationship [41]:

$$d(t) = \begin{cases} 0 & p(t) \le P_0 \\ D(t)\left(\frac{p(t)-P_0}{P_f-P_0}\right)^{0.5} & P_0 \le p(t) \le P_f \\ D(t) & p(t) \ge P_f \end{cases} \quad (1)$$

where D is the desired demand at a node (m^3/s), p is the pressure (m), P_f is the nominal pressure assumed to be 20 m, and P_0 is the lower pressure threshold assumed to be 0 m, below which the consumer cannot receive any water. Accounting for insufficient pressure values is crucial to assess WDS resilience during pipe failures since pressure drops occur as a direct consequence of the additional leak flow. In order to account for these dynamics, the performance of the WDS is assessed using the average satisfied demand:

$$\mathrm{MOP}(t) = \frac{1}{n}\sum_{i=1}^{n}\frac{d_i(t)}{D_i(t)} \quad (2)$$

where n is the total number of demand nodes in the network.

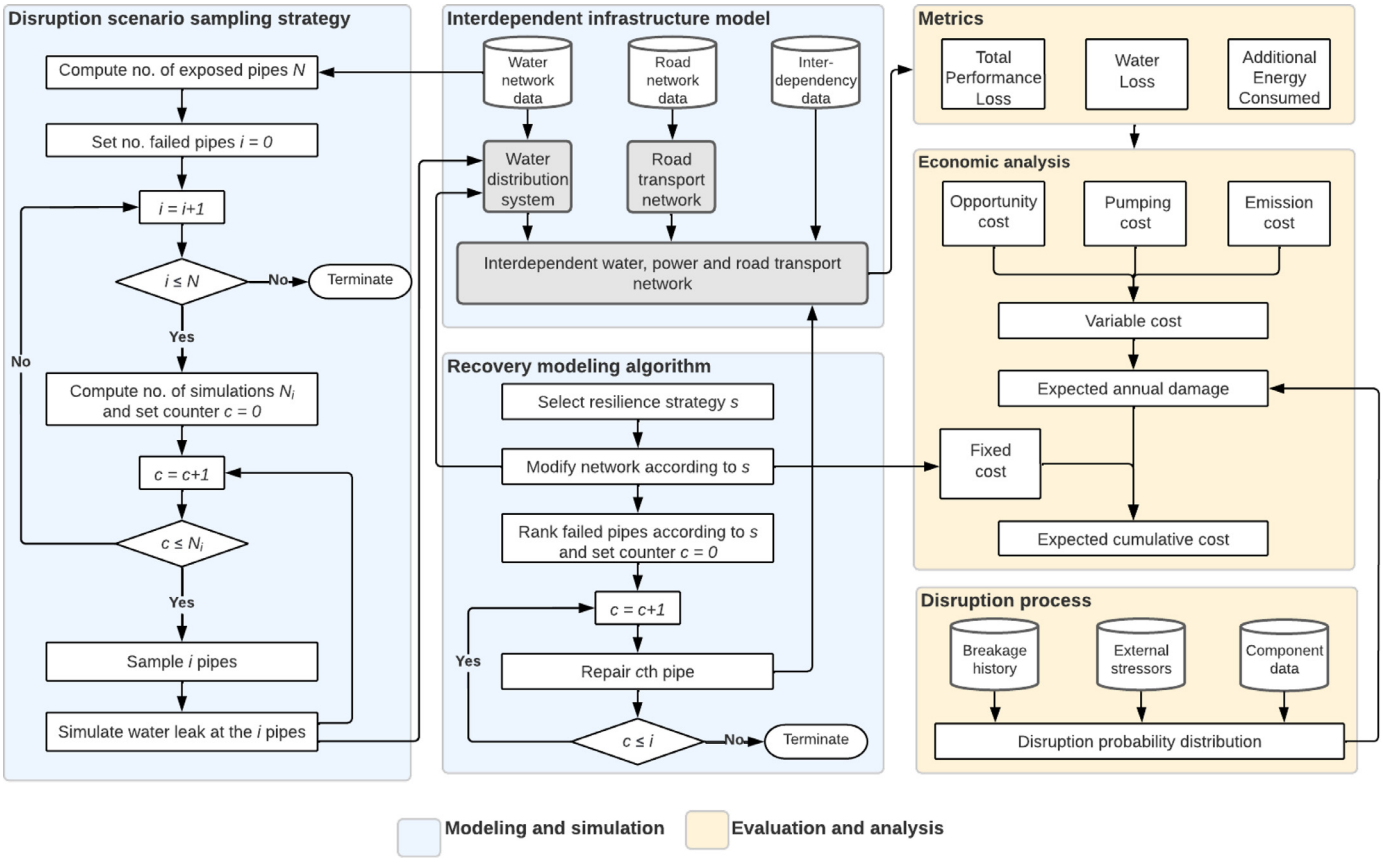

Fig. 1. Methodological framework.

Pipe failure is implemented in the model by splitting the pipe into two segments connected by an artificial leak node, which is then associated with a leak demand. The leak demand at a disrupted pipe i is proportional to the magnitude of the area of the hole (A_i) and the gauge pressure (p_i) [42]:

$$d_i^{leak}(t) = C_d A_i \sqrt{\frac{2p_i(t)}{\rho}} \tag{3}$$

where C_d is the discharge coefficient assumed to be 0.75 (turbulent flow) and ρ is the density of the water. To simulate leakages of various magnitudes, A_i is considered as a random variable [43].

Although the power grid is not explicitly modeled, the interdependency between the water and the power system is modeled in terms of power supplied to water pumps. Specifically, the power supplied to a pump j is computed as the ratio between the hydraulic power (P_h) and the pump efficiency (η assumed to be 0.75):

$$P_j(t) = \frac{P_h(t)}{\eta} = \frac{qh\rho g}{\eta} \tag{4}$$

where q is the flow rate, h is the head gain and g is the acceleration due to gravity.

The road transportation system is explicitly modeled to enable realistic modeling of the dispatch of crews to repair the failed pipes. We assume that road links remain accessible during the disruption and use a static traffic assignment package [44] to implement traffic assignment and compute travel times between origin-destination pairs.

3.1.2. Disruption scenario sampling strategy

Given the high number of pipes exposed to a given hazard (N), considering all the scenarios resulting from the failure of $i = 1, \dots, N$ pipes would be impractical since the entire solution space would be the sum of all the combinations corresponding to each i-level [16]. In order to limit the computational complexity of the problem, and still obtain statistically significant results, we use the two-stage absolute precision method [45] to compute the number of simulations required for each i-level (N_i) in order to achieve a required precision (ϵ):

$$N_i(\epsilon) = \min\left\{ n : n \geq \frac{t^2_{n-1,\alpha} S^2(n_0)}{\epsilon^2}, n \in \mathbb{Z}_+ \right\} \tag{5}$$

where $t^2_{n-1,\alpha}$ is the student-t quantile and $S(n_0)^2$ the sample variance corresponding to initial n_0 simulations [46]. In our case study, the number of simulations N_i is calculated for each i-level assuming $\epsilon = 0.5$ hour, $\alpha = 0.05$ and $n_0 = 50$, and a resilience metric (the total performance loss [hours]) is used to compute $S(n_0)^2$. Using the specified parameters and Eq. (5), the computed number of simulations N_i ensures that the mean total performance loss resulting from the failure of i pipes has 95% confidence interval of 1 h.

3.1.3. Recovery modeling algorithm

A resilience strategy includes modifying the WDS network to improve its resilience and establishing a criterion to determine the repair order of failed components. In this study, we modify the WDS network by closing remotely-controlled shutoff valves in order to isolate the failed pipes. In practice, sensors collect data on pressure heads at remote points in the system and transmit them to the Programmable Logic Controllers (PLCs) associated with the valves. PLCs can implement various preset control logics. For example, if the pressure head is below its design threshold, the PLC sends a control command to the relevant valve actuator in order to shut it off [8,12]. If valves are located at the branch-level, segments of the network containing the failed pipes will be isolated. In this scenario, functional components contained in the isolated segment will also be disconnected from the water sources. If valves are located at the pipe-level, i.e., a pair of valves is associated with each

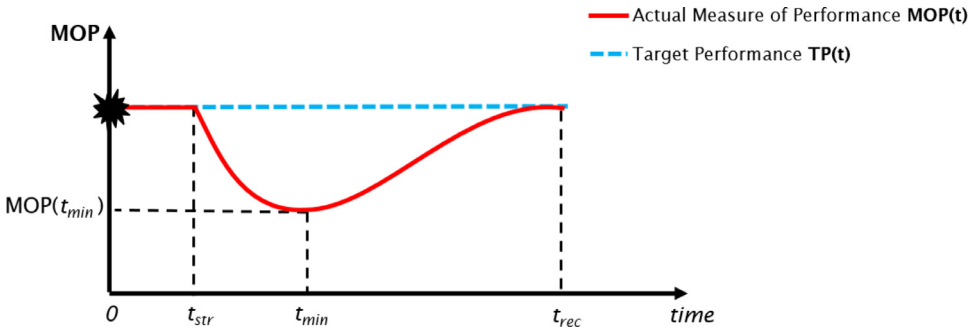

Fig. 2. Recovery cycle.

pipe, only failed pipes will be isolated. In this scenario, functional components remain operative and performance loss is minimized [19].

The recovery strategy remains unchanged across different recovery scenarios. Specifically, pipes with a higher flow are prioritized for repair. The flow for each pipe is calculated by performing a hydraulic simulation during normal operating conditions and assigning to each pipe the maximum daily flow through it. For simplicity but with no loss of generality, a single repair team is responsible for restoring the WDS. Therefore, repair actions are carried out sequentially. Each failed pipe is restored to full functionality after the following actions occur:

1. if remotely controlled shutoff valves are present, valves are shutoff to isolate a failed pipe within 10 minutes of its bursting (this is to resemble a SCADA system),
2. the repair crew reaches the pipe's location by travelling on the road,
3. the failed pipe segment is manually isolated from the network to stop the leak and allow for repair,
4. the failed pipe is repaired and reconnected to the network.

The time taken to restore a single pipe is, therefore, the sum of the crew's travel time from its current location to the failed pipe's location (computed by solving a static traffic assignment problem), the time taken to isolate the pipe (assumed to be 10 minutes) and the time taken to repair and reconnect the pipe (assumed to be proportional to the pipe's diameter, e.g., pipe's diameter [mm]/100 + 2 [hours] [47]). Note that in the base-case scenario, the detection time is considered negligible compared to the total leakage time and is therefore not explicitly modeled [19].

3.2. Evaluation and analysis

3.2.1. Metrics

Fig. 2 represents the recovery cycle, i.e. the system response following a disruption [4,48]. The recovery cycle is determined by different variables, including the external disruption process and the intrinsic capabilities of the system [5]. These include absorptive capability, i.e., the ability to minimize the impacts of disruptions, adaptive capability, i.e., the ability to self-organize for recovery of performance, and recovery capability, i.e., the ability of a system to be repaired [49].

Initially, the system functions at its target performance level TP and is perturbed by an external shock at time $t = 0$. If the system is able to adapt to the shock, performance is maintained within the robustness range and performance loss (or strain) is delayed until $t = t_{str}$ [50]. Subsequently, the system performance drops until it reaches the minimum performance level MOP($t_{\min}$). When the effects of the recovery efforts take place to reduce the consequences of the disruption, system performance may increase and be eventually restored to the initial level TP at $t = t_{rec}$ (as displayed in Fig. 2). However, if the recovery efforts are not sufficient, system performance may not be recovered to the TP level [4].

The system's response to a disruption depends upon the extent to which the system can absorb, adapt to, and recover from it. In order to quantify these capabilities, the total performance loss (TPL) is used [2]:

$$\mathrm{TPL} = \int_{t_{str}}^{t_{rec}} \left[\mathrm{TP}(t) - \mathrm{MOP}(t)\right] dt \tag{6}$$

During a water leakage, water is lost continuously in an amount proportional to the area of the hole and the gauge pressure inside the pipe. In some cases, the water loss due to leaks exceeds 50% of production [51] and inhibits the system's ability to meet demand, especially in areas with high water stress or highly fluctuating water conditions [1]. In order to compensate for the pressure drops due to the leak flow, additional pumping energy is also required to guarantee the minimum operating pressure [52]. The additional energy consumed during water leaks involves an environmental burden in terms of greenhouse gas emissions, acid rain, and resource depletion, among other effects associated with energy production and consumption [51]. For these reasons, accounting for the real water loss (WL) and additional energy consumed (EC) is essential to compare recovery strategies from a sustainability point of view.

WL is equal to the total leak demand (d_{leak}) corresponding to pipe failures during the entire duration of the disruption:

$$\mathrm{WL} = \int_{t_{str}}^{t_{rec}} \sum_i d_i^{leak}(t) dt \tag{7}$$

EC is equal to the difference between the total pumping energy required during disruption and the total pumping energy required during normal operating conditions. Given that the total pumping power is the sum of the power supplied to each pump j during disrupted and normal conditions (denoted by $P_j(t)$ and $P_j^{Target}(t)$, respectively), EC is computed as:

$$\mathrm{EC} = \int_{t_{str}}^{t_{rec}} \left[\sum_j P_j(t) - \sum_j P_j^{Target}(t) \right] dt \tag{8}$$

Note that TPL, WL and EC are computed according to the loss of resilience equation defined in [2] and are inversely proportional to resilience, i.e., the lower the TPL/WL/EC, the higher the resilience.

3.2.2. Economic analysis

An economic analysis of the implemented strategies versus the base-case scenario is conducted in order to assess their costs and benefits in monetary terms. Here, we apply the economic framework developed in [33]. Given that we used synthetic data to create the disruptions, we compute economic losses as a function of the number of failed pipes in the network, rather than the return period as in [33]. The costs associated with each recovery strategy are divided into fixed and variable costs. Fixed costs are associated with the investment required to modify the network according to a specific strategy and any maintenance costs that may derive from it. For the two strategies considered in the case study, investment costs include the costs of pneumatic actuators to control the valves and the cost of new shutoff valves (Table 1). Maintenance and installation costs are assumed negligible.

Table 1
Parameter values for the economic analysis.

Fixed costs		Ref.
Pneumatic actuator	250 $/unit	[53]
Shutoff valve	342 $/unit (51 mm diameter)	[54]
	732 $/unit (102 mm diameter)	
	1733 $/unit (203 mm diameter)	
	3690 $/unit (309 mm diameter)	
Variable costs		**Ref.**
p_w	0.20 $/m^3	[55]
p_e	0.14 $/KWh	[27]
k_{CO2}	1.04 Kg/KWh	[27]
p_{CO2}	0.068 $/Kg	[56]

Variable costs have three components, namely, the opportunity costs of demand not served, the energy costs related to water pumping [52], and possible costs of CO2 emissions (assuming that a carbon tax is enforced [27]). The opportunity cost is the product of the total performance loss (TPL) - computed as in Eq. (6) where TP and MOP are in absolute terms - and the average water price (p_w), the pumping cost is the product of the additional energy consumed (EC) and the average energy price (p_e), and the CO2 emission cost is the product of EC, the amount of CO2 emitted per kWh (k_{CO2}) (assuming all energy is produced from fossil fuel sources) and the price of CO2 emissions (p_{CO2}). Therefore, the variable cost can be computed as:

$$\text{Variable cost} = \text{TPL} \cdot p_w + \text{EC} \cdot p_e + \text{EC} \cdot k_{CO2} \cdot p_{CO2} \tag{9}$$

where the values of the parameters p_w, p_e, k_{CO2} and p_{CO2} are assumed as in Table 1.

In order to compute variable costs on an annual basis, the expected annual damage (EAD) is used as risk indicator to reflect the adverse effect of a given hazard in monetary terms [57]:

$$\text{EAD}(t) = \int_y \text{Variable cost}(y)\ f(y;t)\ dy \tag{10}$$

where y is the disruption (no. of failed pipes) and f the probability density function associated with the disruption process, which varies (i.e., increases) over time to resemble the aging process of the system.

To compare the costs associated with different scenarios, the expected cumulative cost (ECC) over the investment lifecycle is computed as:

$$\text{ECC}(t) = \int_{u=0}^{t} \Big(\text{Fixed cost}(u) + \text{EAD}(u)\Big) du \tag{11}$$

Based on the ECC, the time of break-even can be computed as:

$$\min t\ :\ \text{ECC}_{\text{resilience strategy}}(t) \geq \text{ECC}_{\text{base-case}}(t) \tag{12}$$

3.2.3. Disruption process

To compute the EAD in Eq. (10), a probability density function f is defined to represent the disruption process. The Non-Homogeneous Poisson Process (NHPP) is a common model used for pipe failure modeling, where the hazard rate λ is a function of time, i.e., $\lambda(t)$ [58]. Various hazard rate models have been used in the literature which include additional covariates such as breakage history, material, diameter, length and external stressors, e.g., soil type and overhead traffic conditions [59,60]. The functional form of such models is typically power law, linear, or log-linear. Among these models, the power law model with covariates is most commonly discussed in the literature:

$$\lambda(t) = \lambda\delta t^{\delta-1} \exp\Big(\sum_{i=0}^{n} \beta_i z_i\Big), \quad \text{for } \lambda, \delta > 0 \text{ and } t \geq 0 \tag{13}$$

where $\{z_i, i = 1, \ldots, n\}$ is the set of covariates and $\beta_i, i = 1, \ldots, n$ the estimated coefficients. A repairable system modeled by the power law model is improving if $0 < \delta < 1$ and deteriorates if $\delta > 1$.

Assuming independent hazard processes for different pipes $\lambda_p, p = 1, \ldots, P$, the mean failure rate $\Lambda(t)$ can be computed as follows:

$$\Lambda(t) = \sum_{p=0}^{P} \lambda_p(t) \tag{14}$$

Therefore, the probability of exactly n failures occurring in the time window $(0, t)$ for the NHPP is given by [61]:

$$P(n) = \frac{1}{n!}\Big(\int_0^t \Lambda(u)du\Big)^n \exp\Big(\int_0^t \Lambda(u)du\Big) \tag{15}$$

4. Case study

4.1. Infrastructure network and resilience strategies

We use the synthetic city of Micropolis as a case study (Fig. 3a). Micropolis is a realistic urban infrastructure testbed developed by Texas A&M University [17] consisting of commercial, residential, and industrial units covering an area of approximately five square kilometres. It is a digitally mapped small city of approximately 5000 residents complete with infrastructure information including a complete water system, power network, roads, land parcels, buildings, and topography. The city is traversed by two water streams from north to south. The WDS consists of 1574 demand nodes, 1415 pipes and 196 branch-level shutoff valves. The pipes are classified as main pipes, which are major arterial pipelines, service connector pipes, which connect peripheral demand nodes, and hydrant connectors. Micropolis WDS includes a single water tank and two water sources which provide water supply to the system through a high-service pump station located at the northern edge of the city. The total daily demand for water amounts to 6,087 m^3 and the pumping energy consumption to 2228 KWh (see [17] for a detailed description of Micropolis WDS).

4.2. Disruption scenarios

Various factors may lead to pipe failures, both static (e.g., pipe material, size, soil type) and dynamic (e.g., age, weather-related events) [59]. For example, flash flood events due to overflow of the main water stream during periods of heavy rain may cause rupture of the water pipelines [62]. Previous studies show that pipe failures may occur as a consequence of high soil moisture deficit [63], hydrodynamic forces of the flowing water and/or fatigue failure due to vortex-induced vibrations [64]. The explicit modeling of the relationship between these factors and subsequent pipe failure is out of the scope of this study and relies instead on a few simplifying assumptions. Because main water pipes in the vicinity of the river are more prone to failure due to greater external stressors applied to them, without loss of generality we only consider disruption scenarios involving failure of these exposed pipes (i.e., pipes located within 50 m of the main water stream). Additionally, we solely take into account the breakdown of main pipes that exceed a diameter of 50 mm. This is due to the fact that the failure of smaller pipes, although more frequent, has a negligible impact on the WDS performance, which does not warrant the installation of shutoff valves and their associated actuators.

Pipe bursts are modeled using Eq. (3), where the area of the hole (A_i) is assumed to be uniformly distributed over the range of 1 to 100% of the cross-sectional area of the pipe. Disruptions of increasing magnitude are simulated by increasing the number of failed pipes from 1 to 21 (i.e., the total number of main pipelines exposed, in red in Fig. 3b) according to the sampling strategy described in Subsection 3.1.2.

4.3. Resilience strategies

The Micropolis WDS is provided with branch-level shutoff valves. These valves are placed to resemble a realistic and imperfect system [17]. Moreover, we assume that an incomplete SCADA system is already

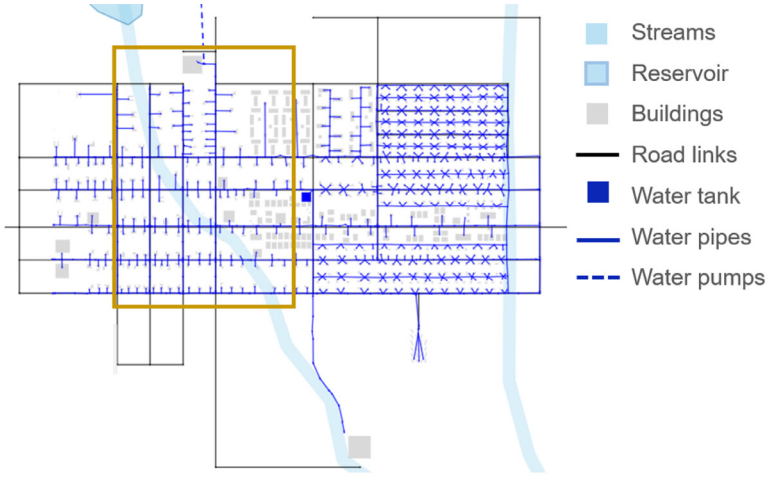

(a) Micropolis water and transportation networks.

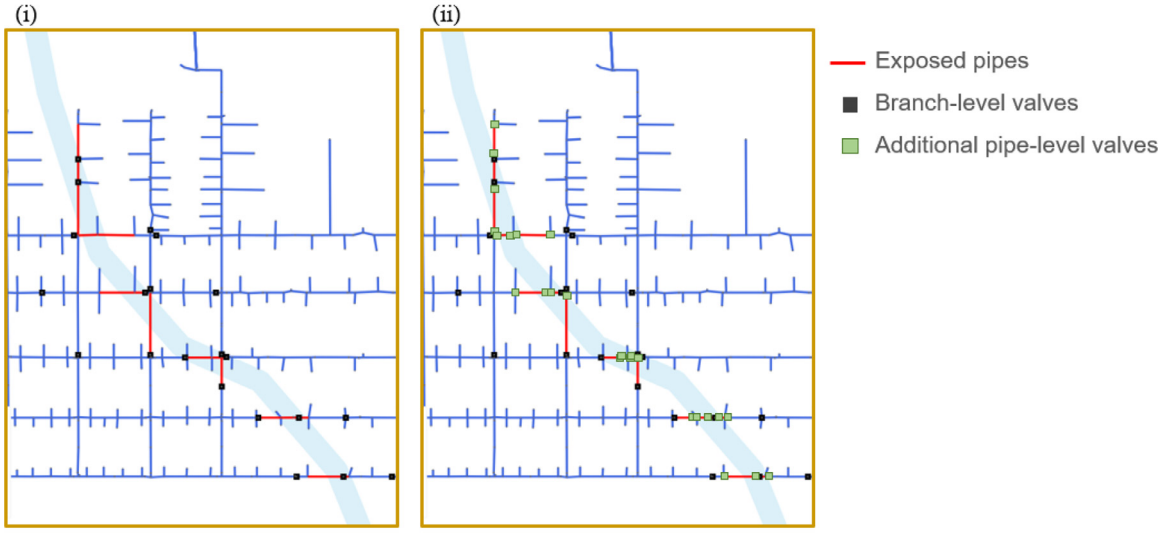

(b) Location of remotely controlled (i) branch-level and (ii) pipe-level valves.

Fig. 3. Micropolis water-transportation network and location of shutoff valves.

present, with sensors and communication systems in place to detect water leakages and transmit alerts to the control center. After leaks are identified, the pipe repair sequence is computed at the control center and the repair crew is dispatched accordingly. Three recovery scenarios are considered, including a base-case scenario in which no resilience strategy is implemented and two structural resilience strategies in which remotely controlled shutoff valves are installed:

1. Base-case scenario. In this scenario, water leaks continue until the repair crew reaches the leakage location and manually isolates the failed pipe segment.
2. Remotely controlled branch-level shutoff valves (Fig. 3b(i)). In this scenario, 21 actuators associated with the existing shutoff valves are installed in order to promptly stop the leakage after its detection (with a delay of 10 minutes). Additional investment is required for the installation of the actuators.
3. Remotely controlled pipe-level shutoff valves (Fig. 3b(ii)). In this scenario, 25 additional shutoff valves (i.e., fifteen 51 mm diameter valves, five 102 mm diameter valves, five 203 mm diameter valves and two 309 mm diameter valves) are installed at the pipe-level in order to avoid the isolation of functional components as in the branch-level shutoff valves scenario (see Section 3.1.3). Furthermore, 42 actuators are installed for each (existing and new) pipe-level shutoff valve. In fact, in order to isolate the 21 exposed pipes, 42 valves (i.e., one at each end of the pipe) and associated actuators need to be installed. Therefore, additional investment is required for the installation of the additional shutoff valves and actuators.

4.4. Costs associated with infrastructure disruptions and resilience strategies

To analyze the results in monetary terms, fixed and variable costs are estimated using Eq. (9) and the parameters reported in Table 1. Furthermore, we assume that the lifespan of the installed actuators and valves is 30 years and that maintenance costs are negligible. The total investment is 5250 $ in the branch-level shutoff valves scenario and 35,335 $ in the branch-level shutoff valves scenario (Table 2).

In the absence of empirical data, we use the hazard rate model estimated by [60] for the city of Trondheim in Norway, which has similar characteristics to Micropolis, including the age and development history. Covariates included in the model are the time from the construction to the beginning of the observation period (assumed to be 2020), diameter, length, and indication of whether the pipe is laid in deposits

Table 2
Fixed costs for the two considered resilience strategies.

	Remotely controlled branch-level shutoff valves	Remotely controlled pipe-level shutoff valves
Additional shutoff valves	0	27
Cost of additional shutoff valves	0 $	24,835 $
Actuators	21	42
Cost of actuators	5250 $	10,500 $
Total fixed costs	**5,250 $**	**35,335 $**

Table 3
Characteristics of the exposed pipes.

Pipe number	Age [years]	Diameter [mm]	Length [m]	Material
1043	110	51	13.289	GC
523	110	51	3.548	GC
524	110	51	41.134	GC
525	110	51	1.756	GC
526	110	51	13.338	GC
528	110	51	8.071	GC
535	110	51	16.666	GC
536	110	51	17.508	GC
537	110	51	38.795	GC
549	110	51	57.656	GC
550	110	51	6.194	GC
646	70	203	18.203	UDI1
647	70	203	60.977	UDI1
672	70	203	123.042	UDI1
687	70	102	32.967	UDI1
688	70	102	65.081	UDI1
732	70	102	105.729	UDI1
802	40	309	61.557	UDI2
803	40	309	9.400	UDI2
863	40	309	45.586	UDI2
864	40	309	69.629	UDI2

Table 4
Parameter values and covariate coefficients for the hazard rate model.

Material	λ	δ	Length	Diameter	Deposits	Clay	Age
GC	0.016	1.129	0.002	-0.001	0.142	0	-0.001
UDI1	0.027	1.281	0.004	-0.004	0	0.412	-0.008
UDI2	0.002	1.488	0	-0.007	0	-0.020	0.155

or clay. The list of exposed pipes with the description of their characteristics is reported in Table 3.

Different hazard models are considered for different pipe materials. Specifically, three models are used for pipes in grey cast (GC), in ductile iron (UDI1) and in ductile iron with simple protection (UDI2). We assume that GC pipes are laid in deposits and UDI1 and UD2 pipes in clay. The corresponding parameter values and covariate coefficients are reported in Table 4.

5. Results

5.1. Performance curves

The performance curves, expressed as mean (over all simulations) MOP versus time, are represented in Fig. 4 for the three recovery scenarios.

In the base-case scenario (Fig. 4(a)), performance is lost suddenly as a result of the tank being emptied and unable to supply water to the system. The tank is emptied at around 8–10 hours despite the large flow of water supplied by the water reservoir as a result of the extra demand for water deriving from the leaky pipes. Recovery is slow and has an oscillatory behavior, which follows the demand pattern. During nighttime, when the demand for water is low, MOP is higher because a relatively higher percentage of the desired demand can be satisfied.

When the branch-level shutoff valves are closed to isolate leaking pipes (Fig. 4(b)), performance is first lost in a small amount due to the effect of the water leaks being stopped and plateaus until about 12 hours. After this time, the tank is emptied at around 13–15 hours and MOP starts to vary with the demand pattern, as in the base-case scenario. As the number of failed pipes increases, so are the number of valves to be closed. With a high number of valves being closed, the likelihood that network components remain isolated from the rest of the network also increases, as reflected by the steeper performance loss curves for scenarios with a high number of failed pipes. Over the entire duration of the disruption, water flow from the water reservoir and node heads are lower than in the base-case scenario, since some demand nodes remain isolated from the network and therefore the overall water flow from the reservoir towards the system is lower.

When the pipe-level shutoff valves are closed to isolate leaking pipes (Fig. 4(c)), the performance behavior follows the one in the branch-level shutoff valves, with the main difference that performance is quickly restabilized at around 20 hours even in the most severe disruption scenarios. This is because water loss is minimized without affecting functional components and the tank capacity is quickly restored.

5.2. Aggregated metrics

The values of the three metrics TPL, WL and EC for each number of failed pipes are represented in Fig. 5 for the three analyzed scenarios. For each level of disruption, installing shutoff valves results in major improvements in terms of TPL, WL and EC.

Overlaps exist between the TPL envelopes of the base-case scenario and the branch-level shutoff valves scenario when less than 16 pipes are failed (Fig. 5(a)). This shows that closing the original valves does not statistically improve system resilience (measured in terms of TPL) for small disruption scenarios. However, as explained in Subsection 5.1, the mechanisms leading to performance loss are different in the two scenarios. In the base-case scenario, performance is lost as a result of water loss. In the original valve closure scenario, performance is lost as a result of network component isolation. The high variability of the TPL in this scenario is due to the sub-optimal placement of the valves. Indeed, while some pipes are effectively isolated by closing adjacent valves, others require the isolation of a large part of the network. TPL is minimized in the pipe-level shutoff valves scenario.

The two shutoff valve scenarios statistically dominate the base-case scenario in terms of WL (Fig. 5(b)). In fact, closing the valves prevents water loss after the leaks have been detected (10 minutes after their occurrence). Due to the modeling of the two shutoff valve strategies, WL is the same in these two scenarios and nearly zero. Notably, the results of the WL in the base-case scenario closely follow those of the TPL, confirming that performance is lost due to the lack of water availability caused by the water leaks.

In the base-case scenario, more energy is consumed by the pumps in order to pump additional water and compensate for water losses and pressure drops during disruptions (Fig. 5(c)). On the contrary, shutting branch-level valves results in energy savings (i.e., negative values of EC), since the water flow from the reservoir decreases as an effect of demand nodes being isolated from the rest of the network, especially for severe disruptions. In the pipe-level shutoff valve scenario, EC is close to zero,

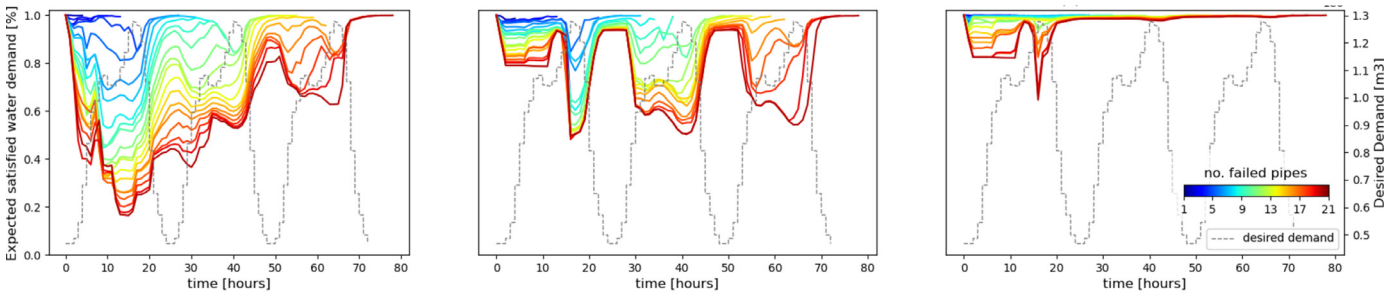

(a) Base-case scenario (b) Branch-level shutoff valves (c) Pipe-level shutoff valves

Fig. 4. Mean Measure of Performance (MOP) versus time in the three analyzed scenarios.

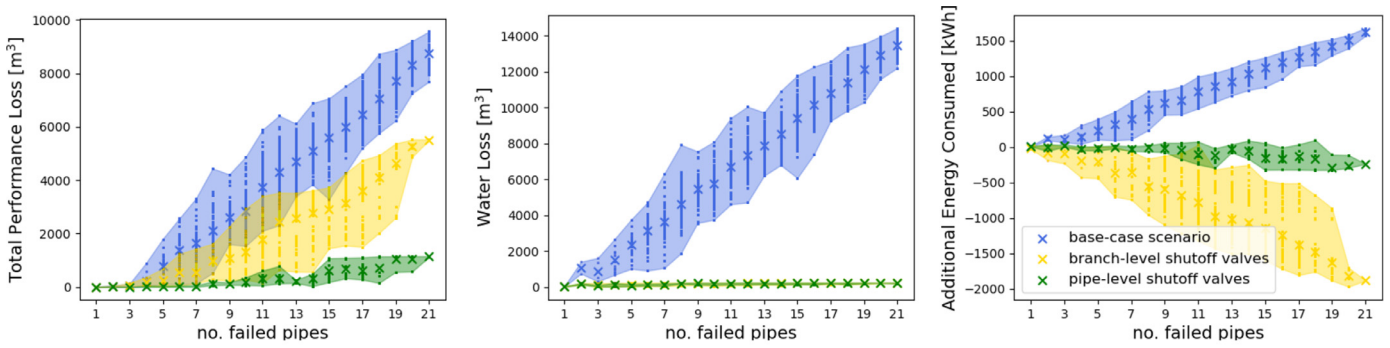

(a) Total Performance Loss (b) Water Loss (branch- and pipe-level shutoff valves scenarios coincide) (c) Additional Energy Consumed

Fig. 5. Metrics versus disruption magnitude (i.e., number of failed pipes).

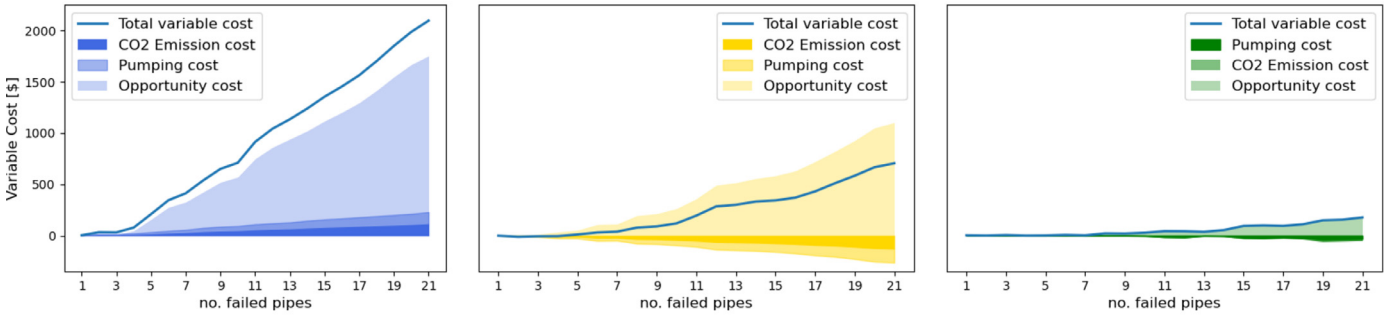

(a) Base-case scenario (b) Branch-level shutoff valves (c) Pipe-level shutoff valves

Fig. 6. Mean variable costs versus disruption magnitude (i.e., number of failed pipes) for the three analyzed scenarios.

since the water pump behavior is close to the behavior during normal operating conditions.

5.3. Expected costs

Fig. 6 shows the variable costs associated with increasing disruption magnitude. In the base-case scenario (Fig. 6(a)), variable costs range from 0 to 2100 $, they are more than halved, i.e., in the range 0 to 705 $, in the branch-level shutoff valves scenario (Fig. 6(b)), also due to the effect of savings resulting from less energy being consumed to pump water into the system, and are almost zero in the pipe-level shutoff valves scenario (Fig. 6(c)). In all scenarios, opportunity costs account for the majority of variable costs.

Due to the assumption of NHPP with $\delta > 1$, the probability of pipe failure increases over time, as reflected by the exponential behavior of the ECC in the three analyzed scenarios (Fig. 7). The higher variable costs in the base case scenarios contribute to the steeper cost curves in Figs. 7(a) and (b). While the time of break-even is 2032 in the branch-level shutoff valves scenario (Fig. 7(a)), it increases to 2043 in the pipe-level shutoff valves scenario (7(b)), due to the higher investment required of installing additional valves. However, the cost savings in the long-term are greater in this scenario.

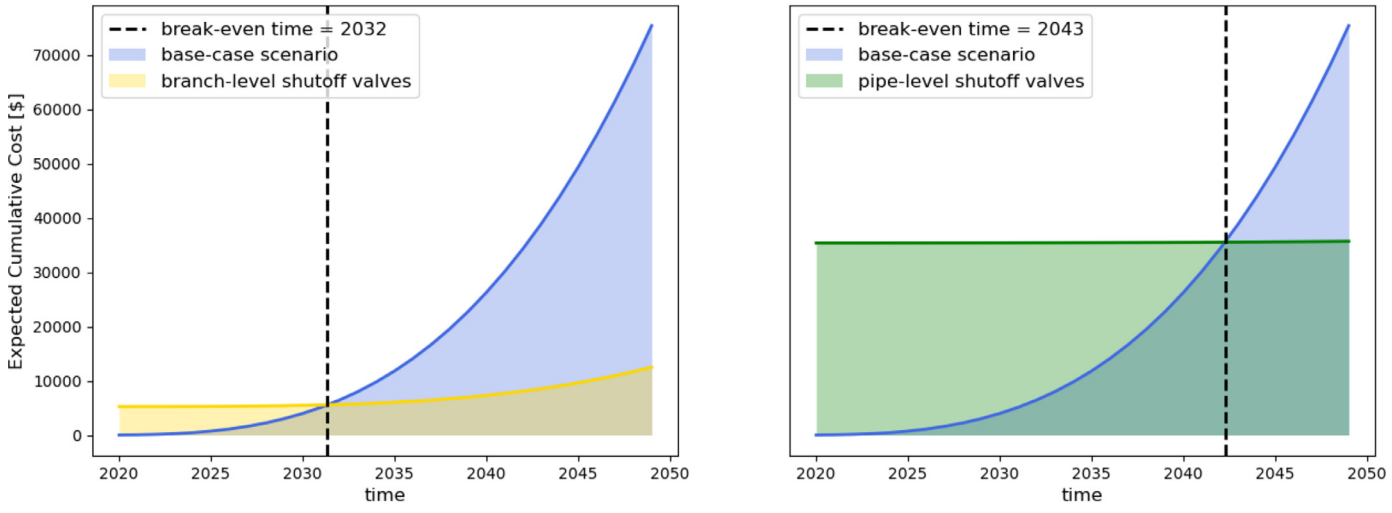

(a) Branch-level shutoff valves (b) Pipe-level shutoff valves

Fig. 7. Economic analyses of the two resilience strategies compared to the base-case scenario.

6. Conclusions

In this paper, we developed a methodological framework to assess the performance of a WDS and its interdependent power and transportation systems under disruption scenarios and two resilience strategies. Three metrics were used to measure the performance of WDS under various conditions, namely total performance loss, water loss and additional energy consumed. An economic analysis based on the monetization of these three metrics was conducted in order to compare the two resilience strategies. In the first resilience strategy, actuators are installed in order to remotely control existing branch-level shutoff valves and promptly isolate network segments containing water leakages. Because existing shutoff valves are located at the branch-level, functional elements contained in the isolated network segments remain disconnected from the water sources. In the second strategy, additional shutoff valves and actuators are installed at the pipe-level in order to remotely isolate leaking pipes. In this scenario, only failed components remain isolated from the water sources. Results show that remotely controlling existing branch-level shutoff valves results in decreased total performance loss, no water loss and energy savings. The best results are obtained when additional shutoff valves at the pipe-level were installed, due to the fact that the total performance loss is further reduced compared to the other scenarios. However, the improved system performance comes at the expense of higher initial investment costs. The economic analysis shows that over time the benefits of reducing the opportunity costs of disruptions outweigh the investment costs. Therefore, when evaluating investments in resilience, system managers and stakeholders must adopt a long-term perspective, which favours low opportunity costs over high returns on investment.

The contribution of our framework lies in the integration of an engineering perspective on resilience and economic analysis in order to evaluate the trade-offs between alternative investments in resilience, hence pricing the desired level of system resilience. Flow-based simulation is used in resilience engineering to accurately represent system performance during disrupted conditions. The economic analysis offers a standardized method to compare multidimensional system performance based on costs. By combining these methods, the trade-offs between different network designs are identified.

Finally, the study presents some limitations and opportunities for further research. First, due to data availability constraints, the framework is showcased with application to the synthetic city of Micropolis. In future research, a real-world case study will be analysed and used for validating the simulation model. Second, the expected costs considered are the costs incurred by the water utility in case of disruption, while the indirect costs associated with water supply interruptions are not considered. In future research, a macro-economic model will be integrated with the infrastructure model in order to quantify the reduction in industrial output due to infrastructure service loss. Third, in order to limit the complexity of the case study, only a few disruption scenarios and two recovery strategies were considered. However, the methodology can be scaled up to test a wider range of disruption scenarios and readily extended to additional case studies. For example, disruptions could be generated using a specific hazard simulator (e.g., earthquake, flood, hurricane) and optimal recovery strategies analyzed (e.g., selective closure of failed pipes to maximize network resilience).

Data Availability

All data and Python scripts used to conduct this study are available on request from the corresponding author.

Relevance to Resilience

This article discusses the problem of critical infrastructure resilience from an engineering perspective and an economic perspective by developing a methodological framework based on system simulation and Cost-Benefit Analysis.

Declaration of competing interest

The authors declare no conflict of interest.

Acknowledgments

The research was conducted at the Singapore-ETH Centre, which was established collaboratively between ETH Zurich and the National Research Foundation Singapore. This research is supported by the National Research Foundation, Prime Minister's Office, Singapore under its Campus for Research Excellence and Technological Enterprise (CREATE) programme.

References

[1] Burek P, Satoh Y, Fischer G, Kahil MT, Scherzer A, Tramberend S, Nava L, Wada Y, Eisner S, Flörke M, et al. Water futures and solution-fast track initiative Tech. Rep.. International Institute for Applied Systems Analysis (IIASA); 2016. https://pure.iiasa.ac.at/id/eprint/13008/

[2] Bruneau M, Chang SE, Eguchi RT, Lee GC, O'Rourke TD, Reinhorn AM, Shinozuka M, Tierney K, Wallace WA, Von Winterfeldt D. A framework to quantitatively assess and enhance the seismic resilience of communities. Earthquake Spectra 2003;19(4):733–52. doi:10.1193/1.1623497.

[3] Hosseini S, Barker K, Ramirez-Márquez JE. A review of definitions and measures of system resilience. Reliab Eng Syst Saf 2016;145:47–61. doi:10.1016/j.ress.2015.08.006.

[4] Cassottana B, Shen L, Tang LC. Modeling the recovery process: a key dimension of resilience. Reliab Eng Syst Saf 2019:106528. doi:10.1016/j.ress.2019.106528.

[5] Shen L, Cassottana B, Heinimann HR, Tang LC. Large-scale systems resilience: a survey and unifying framework. Qual Reliab Eng Int 2020;36(4):1386–401. doi:10.1002/qre.2634.

[6] Haimes YY. On the complex definition of risk: a systems-based approach. Risk Anal: Int J 2009;29(12):1647–54. doi:10.1111/j.1539-6924.2009.01310.x.

[7] Haimes YY. On the definition of resilience in systems. Risk Anal: Int J 2009;29(4):498–501. doi:10.1111/j.1539-6924.2009.01216.x.

[8] Creaco E, Walski T. Economic analysis of pressure control for leakage and pipe burst reduction. J Water Resour Plann Manage 2017;143(12):04017074. doi:10.1061/(ASCE)WR.1943-5452.0000846.

[9] Haider H, Al-Salamah IS, Ghazaw YM, Abdel-Maguid RH, Shafiquzzaman M, Ghumman AR. Framework to establish economic level of leakage for intermittent water supplies in arid environments. J Water Resour Plann Manage 2018;145(2):05018018. doi:10.1061/(ASCE)WR.1943-5452.0001027.

[10] Taormina R, Galelli S, Tippenhauer NO, Ostfeld A, Salomons E. Assessing the effect of cyber-physical attacks on water distribution systems. In: World Environmental and Water Resources Congress 2016; 2016. p. 436–42. doi:10.1061/9780784479865.046.

[11] Taormina R, Galelli S, Tippenhauer NO, Salomons E, Ostfeld A. Characterizing cyber-physical attacks on water distribution systems. J Water Resour Plann Manage 2017;143(5):04017009. doi:10.1061/(ASCE)WR.1943-5452.0000749.

[12] Creaco E, Campisano A, Fontana N, Marini G, Page P, Walski T. Real time control of water distribution networks: astate-of-the-art review. Water Res 2019;161:517–30. doi:10.1016/j.watres.2019.06.025.

[13] Housh M, Ohar Z. Model-based approach for cyber-physical attack detection in water distribution systems. Water Res 2018;139:132–43. doi:10.1016/j.watres.2018.03.039.

[14] Jin AS, Trump BD, Golan M, Hynes W, Young M, Linkov I. Building resilience will require compromise on efficiency. Nat Energy 2021:1–3. doi:10.1038/s41560-021-00913-7.

[15] Diao K, Sweetapple C, Farmani R, Fu G, Ward S, Butler D. Global resilience analysis of water distribution systems. Water Res 2016;106:383–93. doi:10.1016/j.watres.2016.10.011.

[16] Mugume SN, Gomez DE, Fu G, Farmani R, Butler D. A global analysis approach for investigating structural resilience in urban drainage systems. Water Res 2015;81:15–26. doi:10.1080/1573062X.2016.1253754.

[17] Brumbelow K, Torres J, Guikema S, Bristow E, Kanta L. Virtual cities for water distribution and infrastructure system research. In: World environmental and water resources congress 2007: Restoring our natural habitat; 2007. p. 1–7.

[18] Holling CS. Resilience and stability of ecological systems. Annu Rev Ecol Syst 1973;4(1):1–23. https://www.jstor.org/stable/2096802

[19] Paez D, Filion Y, Castro-Gama M, Quintiliani C, Santopietro S, Sweetapple C, et al. Battle of postdisaster response and restoration. J Water Resour Plann Manage 2020;146(8):04020067.

[20] Chelleri L, Waters JJ, Olazabal M, Minucci G. Resilience trade-offs: addressing multiple scales and temporal aspects of urban resilience. Environ Urban 2015;27(1):181–98. doi:10.1177/0956247814550780.

[21] Anderies JM, Folke C, Walker B, Ostrom E. Aligning key concepts for global change policy: robustness, resilience, and sustainability. Ecol Soc 2013;18(2). doi:10.5751/ES-05178-180208.

[22] Elmqvist T, Andersson E, Frantzeskaki N, McPhearson T, Olsson P, Gaffney O, Takeuchi K, Folke C. Sustainability and resilience for transformation in the urban century. Nature Sustain 2019 2:4 2019;2(4):267–73. doi:10.1038/s41893-019-0250-1.

[23] Elmqvist T. Development: sustainability and resilience differ. Nature 2017;546(7658). doi:10.1038/546352d. 352–352

[24] Linkov I, Bridges T, Creutzig F, Decker J, Fox-Lent C, Kröger W, et al. Changing the resilience paradigm. Nat Clim Chang 2014;4(6):407–9. doi:10.1038/nclimate2227.

[25] Chang SE, Shinozuka M. Measuring improvements in the disaster resilience of communities. Earthquake Spectra 2004;20(3):739–55. doi:10.1193/1.1775796.

[26] Battle of water networks. 2022. Accessed = 2022-12-30, https://wdsa-ccwi2022.upv.es/battle-of-water-networks/.

[27] Salomons E, Ostfeld A, Kapelan Z, Zecchin A, Marchi A, Simpson A. The battle of the water networks II. In: 14th Water Distribution Systems Analysis Conference (WDSA 2012); Engineers Australia: Adelaide, Australia; 2012.

[28] Marchi A, Salomons E, Ostfeld A, Kapelan Z, Simpson AR, Zecchin AC, et al. Battle of the water networks II. J Water Resour Plann Manage 2014;140(7):04014009. doi:10.1061/(ASCE)WR.1943-5452.0000378.

[29] Nyahora PP, Babel MS, Ferras D, Emen A. Multi-objective optimization for improving equity and reliability in intermittent water supply systems. Water Supply 2020;20(5):1592–603. doi:10.2166/ws.2020.066.

[30] Prasad TD, Park N-S. Multiobjective genetic algorithms for design of water distribution networks. J Water Resour Plann Manage 2004;130(1):73–82. doi:10.1061/(ASCE)0733-9496(2004)130:1(73).

[31] Dandy GC, Engelhardt M. Multi-objective trade-offs between cost and reliability in the replacement of water mains. J Water Resour Plann Manage 2006;132(2):79–88. doi:10.1061/(ASCE)0733-9496(2006)132:2(79).

[32] Suribabu C. Resilience-based optimal design of water distribution network. Appl Water Sci 2017;7(7):4055–66. doi:10.1007/s13201-017-0560-2.

[33] Zhou Q, Mikkelsen PS, Halsnæs K, Arnbjerg-Nielsen K. Framework for economic pluvial flood risk assessment considering climate change effects and adaptation benefits. J Hydrol (Amst) 2012;414:539–49. doi:10.1016/j.jhydrol.2011.11.031.

[34] Chang SE, Svekla WD, Shinozuka M. Linking infrastructure and urban economy: simulation of water-disruption impacts in earthquakes. Environ Plan B: Plann Des 2002;29(2):281–301. doi:10.1068/b2789.

[35] Cimellaro GP, Reinhorn AM, Bruneau M. Seismic resilience of a hospital system. Struct Infrastruct Eng 2010;6(1–2):127–44. doi:10.1080/15732470802663847.

[36] Baroud H, Barker K, Ramirez-Marquez JE, Rocco CM. Inherent costs and interdependent impacts of infrastructure network resilience. Risk Anal 2015;35(4):642–62. doi:10.1111/risa.12223.

[37] Hwang HH, Lin H, Shinozuka M. Seismic performance assessment of water delivery systems. J Infrastruct Syst 1998;4(3):118–25. doi:10.1061/(ASCE)1076-0342(1998)4:3(118).

[38] Klise KA, Bynum M, Moriarty D, Murray R. A software framework for assessing the resilience of drinking water systems to disasters with an example earthquake case study. Environ Modell Softw 2017;95:420–31. doi:10.1016/j.envsoft.2017.06.022.

[39] Creaco E, Di Nardo A, Iervolino M, Santonastaso G. High-order global algorithm for the pressure-driven modeling of water distribution networks. J Water Resour Plann Manage 2022;148(3):04021109.

[40] Todini E, Farina A, Gabriele A, Gargano R, Rossman L. Comparing alternative pda solvers with epanet. J Hydroinf 2022;24(3):697–710.

[41] Wagner JM, Shamir U, Marks DH. Water distribution reliability: simulation methods. J Water Resour Plann Manage 1988;114(3):276–94. doi:10.1061/(ASCE)0733-9496(1988)114:3(276).

[42] Crowl DA, Louvar JF. Chemical process safety: fundamentals with applications. Pearson Education; 2001.

[43] Hagos M, Jung D, Lansey KE. Optimal meter placement for pipe burst detection in water distribution systems. J Hydroinf 2016;18(4):741–56. doi:10.2166/hydro.2016.170.

[44] Boyles SD, Lownes NE, Unnikrishnan A. Transportation network analysis, vol 1. 085; 2020.

[45] Nakayama MK. Two-stage stopping procedures based on standardized time series. Manage Sci 1994;40(9):1189–206.

[46] Balakrishnan S, Zhang Z. Modeling interdependent effects of infrastructure failures using imprecise dependency information. Sustain Resilient Infrastruct 2020:1–17. doi:10.1080/23789689.2020.1735836.

[47] Choi J, Yoo DG, Kang D, et al. Post-earthquake restoration simulation model for water supply networks. Sustainability 2018;10(10):3618. doi:10.3390/su10103618.

[48] Cassottana B, Aydin NY, Tang LC. Quantitative assessment of system response during disruptions: an application to water distribution systems. J Water Resour Plann Manage 2021;147(3):04021002. doi:10.1061/(ASCE)WR.1943-5452.0001334.

[49] Vugrin ED, Warren DE, Ehlen MA. A resilience assessment framework for infrastructure and economic systems: quantitative and qualitative resilience analysis of petrochemical supply chains to a hurricane. Process Saf Prog 2011;30(3):280–90. doi:10.1002/prs.10437.

[50] Woods DD. Four concepts for resilience and the implications for the future of resilience engineering. Reliab Eng Syst Saf 2015;141:5–9. doi:10.1016/j.ress.2015.03.018.

[51] Ávila CAM, Sánchez-Romero F-J, López-Jiménez PA, Pérez-Sánchez M. Leakage management and pipe system efficiency. its influence in the improvement of the efficiency indexes. Water (20734441) 2021;13(14). doi:10.3390/w13141909.

[52] Colombo AF, Karney BW. Impacts of leaks on energy consumption in pumped systems with storage. J Water Resour Plann Manage 2005;131(2):146–55. doi:10.1061/(ASCE)0733-9496(2005)131:2(146).

[53] C series pneumatic valve actuator. https://assuredautomation.com/C-pneumatic-actuators/C-pneumatic-valve-actuator-price-list.php; Accessed: 2022-07-14.

[54] Economy wedge gate valve series. Accessed: 2022-07-14, https://assuredautomation.com/WCB-150-wedge-gate-valves/index.php.

[55] Holidu. Lowest prices of tap water in selected cities worldwide in 2021. 2021. Accessed = 2022-12-30, https://www.statista.com/statistics/478888/leading-cities-based-on-lowest-freshwater-prices/.

[56] OECD. Effective carbon rates 2021: pricing carbon emissions through taxes and emissions trading. OECD Publisihng; 2021. https://www.oecd-ilibrary.org/content/publication/0e8e24f5-en

[57] Merz B, Elmer F, Thieken A. Significance of "high probability/low damage" versus "low probability/high damage" flood events. Nat Hazards Earth Syst Sci 2009;9(3):1033–46. doi:10.5194/nhess-9-1033-2009.

[58] Scheidegger A, Leitao JP, Scholten L. Statistical failure models for water distribution pipes–a review from a unified perspective. Water Res 2015;83:237–47. doi:10.1016/j.watres.2015.06.027.

[59] Liu Z, Kleiner Y, Rajani B, Wang L, Condit W. Condition assessment technologies for water transmission and distribution systems. Tech. Rep.. United States Environmental Protection Agency (EPA); 2012.

[60] Røstum J. Statistical modelling of pipe failures in water networks. Fakultet for ingeniørvitenskap og teknologi; 2000.

[61] Todinov M. 6 - Losses from failures for repairable systems with components logically arranged in series. In: Todinov M, editor. Risk-Based Reliability Analysis and Generic Principles for Risk Reduction. Oxford: Elsevier; 2007. p. 121–34. doi:10.1016/B978-008044728-5/50006-8.

[62] Arrighi C, Tarani F, Vicario E, Castelli F. Flood impacts on a water distribution network. Nat Hazards Earth Syst Sci 2017;17(12):2109–23. doi:10.5194/nhess-17-2109-2017.

[63] Barton NA, Farewell TS, Hallett SH. Using generalized additive models to investigate the environmental effects on pipe failure in clean water networks. npj Clean Water 2020;3(1):1–12. doi:10.1038/s41545-020-0077-3.

[64] Morse T.L., Mathierson E., Shrestha P.L.P.. The dangers of flood scouring on buried pipeline river crossings. 2017. Accessed: 2022-07-14, https://www.exponent.com/knowledge/alerts/2017/04/flood-scouring-on-buried-pipeline/?pageSize=NaN&pageNum=0&loadAllByPageSize=true.